

Simulation of photon density distribution in three section DBR tunable laser diode based on the transfer matrix method

M. H. Yavari^a, *V. Ahmadi^{a, b}, A. Zarifkar^c, K. Abedi^{a, b}

^aDept. of Elect. Eng., Tarbiat Modares University, Tehran, Iran

^bLaser Research Center, AEOI, Tehran, Iran

^cIran Telecommunication Research Center, Tehran, Iran

ABSTRACT

A model based on the transfer matrix method (TMM), for the analysis of photon density distribution in three section distributed Bragg reflector (DBR) Tunable Laser Diode, is presented. The key feature of the model is the use of modified oscillation condition. This model provides longitudinal distribution of photon density in each section of laser for different values of grating and phase current. It is shown that both grating and phase current caused to a downward shift of photon density distribution profile. Simulation shows that, photon density distribution has peak at the active-passive interface.

Keywords: Tunable Semiconductor Laser, Transfer Matrix Method, Wavelength Division Multiplexing (WDM)

1. INTRODUCTION

Tunable semiconductor lasers are attractive for a variety of applications in optical communications, such as dense WDM, local oscillator tuning in coherent optical communication systems, and optical switching in local area networks [1-4]. The critical point, in the analysis of tunable laser diodes is the tracing of dominant oscillating mode. Several works have been done on the theory of wavelength tuning in multielectrode DBR lasers [5-11]. The previous works on the static characteristics of three-section DBR device by Pan *et al.* [6], Patzak *et al.* [7] Caponio *et al.* [8] have been extended by Tsigopoulos *et al.* [9], however the effect of active-passive interface in oscillation condition is not considered. In our previous work [12], we describe a detailed model with modified oscillation condition which considers the effect of discontinuity and misalignment at the active-passive interface, with exact oscillating condition, static characteristics such as threshold current, output power, oscillating wavelength were obtained and the effects of a discontinuity at the active-passive interface and also the manufacturing imperfections on the device characteristics were investigated. In this study we used our previous results [12-13] and with exact oscillation condition, we simulate photon density distribution in three section DBR tunable laser diode.

The paper organized as follows: In section 2, the theory of the model is presented. In section 3, the relation for calculation of electric field, in each laser section is stated. The results are discussed in section 4 and finally, conclusion is brought in section 5.

2. LASER STRUCTURE AND THEORY OF ANALYSIS

The structure of a three-section DBR laser is shown in Fig. 1. It consists of three longitudinally integrated waveguide sections: an active Fabry-Perot section providing the optical gain for the laser operation, a passive phase control (PC) section which contains neither gratings nor active material and a passive DBR mirror section. The three sections have separate electrodes and are assumed electrically isolated from each other. By injecting current into one of the passive sections, the carrier density increases which leads to a decrease of the refractive index due to the free-carrier plasma effect and a subsequent increase of the Bragg frequency.

* Corresponding Author:

Dept. of Elect. Eng., Tarbiat Modares University

P.O. BOX 14115-143, Tehran, Iran.

E-mail: v_ahmadi@modares.ac.ir

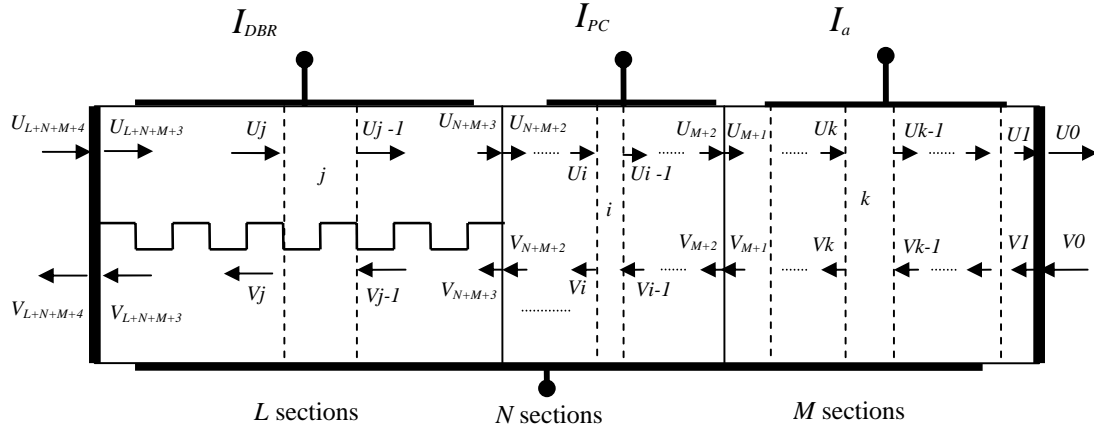


Figure 1: Schematic diagram of three section DBR tunable laser diode for computing photon density distribution in each laser section ($M=11$, $N=10$, $L=1990$)

2.1 Modification of oscillation condition

Modification is based on the transfer matrix method (TMM) [14-18], transmission line [19-20] and scattering theory [17]. By considering the active-passive interface, and using transmission line theory, we obtain the modified oscillation condition for the lasing modes:

$$\frac{(S_{11}S_{22} - S_{12}S_{21}) \cdot r_{DBR} e^{-j2\tilde{\beta}_2 L_2} - S_{11} \cdot r_1 \cdot e^{-j2\tilde{\beta}_1 L_1}}{S_{22} r_{DBR} e^{-j2\tilde{\beta}_2 L_2} - 1} = 1 \quad (1)$$

where L_1 and L_2 are the length of active and passive section respectively. r_{DBR} is the effective reflectivity of the DBR section including the reflectivity at the right facet and r_1 is the facet reflectivity at the left end of the structure. S_{11} , S_{22} , S_{12} and S_{21} are the elements of scattering matrix at the interface between active-passive section [9].

$$S_{11} = \frac{\bar{n}_1 - \bar{n}_2}{\bar{n}_1 + \bar{n}_2} + R \quad (2)$$

$$S_{22} = \frac{\bar{n}_2 - \bar{n}_1}{\bar{n}_1 + \bar{n}_2} - R' \quad (3)$$

$$S_{21} = \frac{\sqrt{2R(\bar{n}_1 + \bar{n}_2)(\bar{n}_2 - \bar{n}_1) - R^2(\bar{n}_1 + \bar{n}_2)^2 - |C_L|^2(\bar{n}_1 + \bar{n}_2)^2 + 4\bar{n}_1\bar{n}_2}}{(\bar{n}_1 + \bar{n}_2)} \quad (4)$$

S_{12} is given by expression (4) if one replaces R by R' . \bar{n}_1 and \bar{n}_2 are the refractive index of active and passive sections, respectively. $|C_L|^2$ expresses the amount of energy lost at interface. R and R' represent the additional reflection due to the waveguide misalignment at the active-passive interface and are also input parameters to the model. The complex wave numbers for the three sections are given by

$$\tilde{\beta}_1(\omega, N_1) = \frac{\omega}{c} \bar{n}_1(\omega, N_1) + \frac{j}{2} [\Gamma_1 g_1(\omega, N_1) - \alpha_1(N_1)] \quad (5)$$

$$\tilde{\beta}_i(\omega, N_i) = \frac{\omega}{c} \bar{n}_i(\omega, N_i) - \frac{j}{2} \alpha_i(N_i) = \frac{\omega}{c} [\bar{n}_0 + \Delta \bar{n}_i(N_i)] - \frac{j}{2} [\alpha_0 + \Delta \alpha_i(N_i)], \quad (i=2,3) \quad (6)$$

c is the light velocity in vacuum, Γ_1 is the confinement factor of the active section, ω is the angular optical frequency; N_1 , N_2 , and N_3 are the carrier densities in the active, the phase and the DBR sections. \bar{n}_1 and α_1 are the effective refractive index and internal absorption of the active section, \bar{n}_2 and \bar{n}_3 are the effective refractive indexes of the phase and DBR sections. ω is the frequency of oscillation, $g_1(\omega, N_1)$ is the modal gain of the active section, and \bar{n}_0 and α_0 are the effective refractive index and internal absorption of the passive sections in the absence of carrier injection. The carrier-induced index and absorption changes are expressed as [6], [9], [19].

$$\Delta \bar{n}_i(N_i) = \Gamma \frac{dn}{dN} N_i \quad (7)$$

$$\Delta \alpha_i(N_i) = \Gamma \frac{d\alpha}{dN} N_i \quad (8)$$

where Γ is the confinement factor, and dn/dN and $d\alpha/dN$ are material parameters. The characteristic equation (1) is separated in its real and imaginary parts:

$$\begin{aligned} -\xi \cdot r_1 |r_{DBR}| \exp(2\alpha_{th}L_1 - \alpha_2L_2) \cdot \sin \left[2 \left(\frac{\omega \bar{n}_1 L_1}{c} + \frac{\omega \bar{n}_2 L_2}{c} - \frac{\varphi}{2} \right) \right] \\ = -S_{11} r_{ap} r_1 \exp(2\alpha_{th}L_1) \sin \left(2 \frac{\omega \bar{n}_2 L_2}{c} \right) + S_{22} \cdot |r_{DBR}| \exp(-\alpha_2L_2) \sin \left[2 \left(\frac{\omega \bar{n}_2 L_2}{c} - \frac{\varphi}{2} \right) \right] \end{aligned} \quad (9)$$

$$\begin{aligned} 1 + \xi \cdot r_1 |r_{DBR}| \exp(2\alpha_{th}L_1 - \alpha_2L_2) \cdot \cos \left[2 \left(\frac{\omega \bar{n}_1 L_1}{c} + \frac{\omega \bar{n}_2 L_2}{c} - \frac{\varphi}{2} \right) \right] \\ = S_{11} \cdot r_1 \exp(2\alpha_{th}L_1) \cos \left(2 \frac{\omega \bar{n}_2 L_2}{c} \right) + S_{22} \cdot |r_{DBR}| \exp(-\alpha_2L_2) \cos \left[2 \left(\frac{\omega \bar{n}_2 L_2}{c} - \frac{\varphi}{2} \right) \right] \end{aligned} \quad (10)$$

where $r_{ap} = (\bar{n}_1 - \bar{n}_2) / (\bar{n}_1 + \bar{n}_2)$, $r_{DBR} = |r_{DBR}| \exp(j\varphi)$, $\xi = S_{11}S_{22} - S_{12}S_{21}$, $\alpha_{th} = (\Gamma_1 g_1(\omega, N_1) - \alpha_1(N_1)) / 2$. In the case when $C_L = 0$, $R = 0$, $R' = 0$ then $\xi = -1$, $S_{22} = -r_{ap}$, $S_{11} = r_{ap}$ and the above equations coincide with the oscillation conditions given by Tsigopoulos *et al* [9] and when $\bar{n}_1 = \bar{n}_2$ and the effect of misalignment is neglected, the above equation leads to the oscillation conditions given by Pan *et al* [6]. When $\bar{n}_1 \neq \bar{n}_2$, $C_L \neq 0$, $R \neq 0$ and $R' \neq 0$ the equations presented in [6] and [9] give only an approximation of (9) and (10). In general case, one has to solve simultaneously the complex relations (9) and (10) numerically, with respect to ω and α_{th} in order to find the oscillation conditions $(\omega^m, \alpha_{th}^m)$ of the m_{th} mode.

2.2 Bragg Grating Section Model

The Bragg grating section can be modeled by interpreting grating structures with transfer matrix [12]. The basis of the TMM is to divide each laser section, longitudinally into a number of sections where the structural and material parameters are assumed to be homogeneous throughout each section. Each of the sections is characterized by its own 2×2 complex transfer matrix that modifies the forward and backward traveling-wave amplitudes as they propagate through the section. The transfer matrices associated with the elementary subsections can normally be found in a straightforward manner. Fig. 2 shows the most basic transmission matrices associated with a homogeneous waveguide of length L with a complex propagation constant $\tilde{\beta}$ [Fig. 2(a)], a refractive index step from n_1 to n_2 [Fig. 2(b)] and one period of grating [Fig. 2(c)]. From these structures it is possible to build a wide range of laser structures [9].

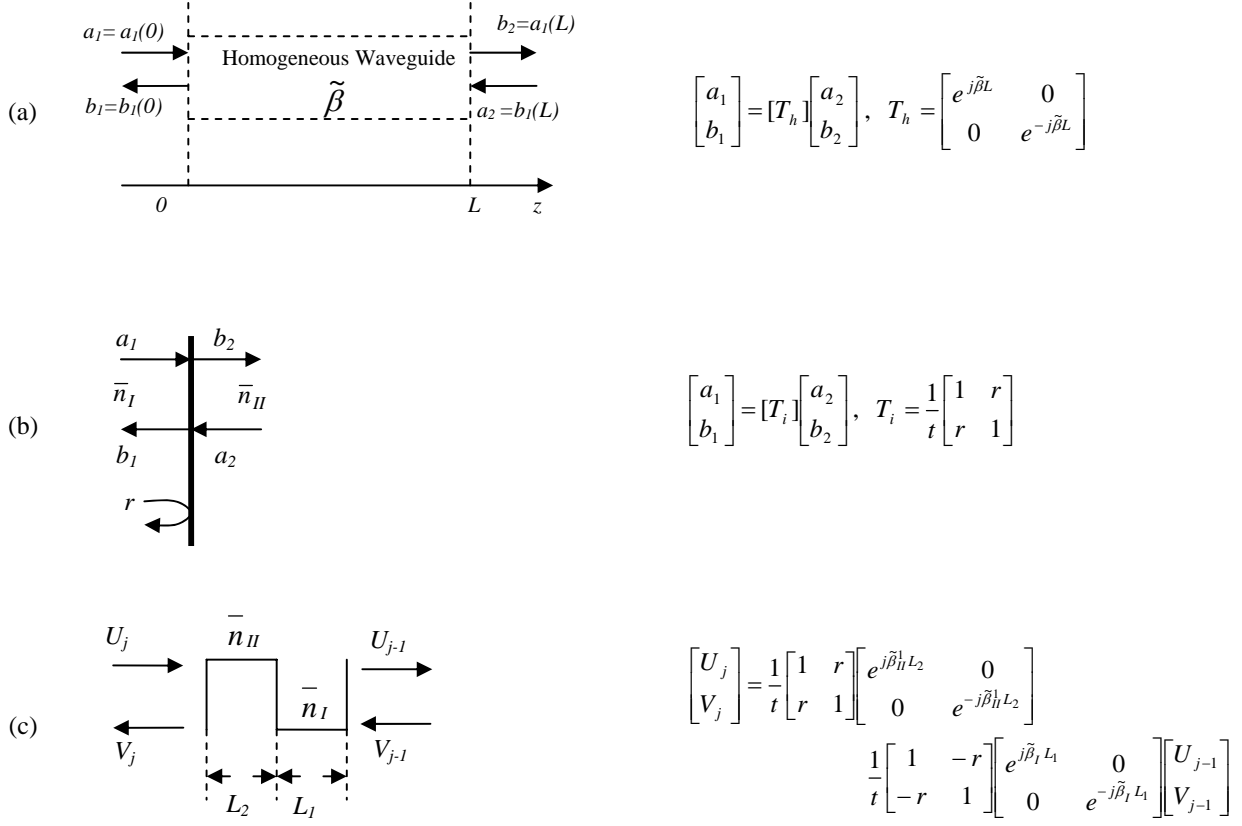


Figure 2: Basic transmission matrices for (a) homogeneous waveguide, (b) refractive index step, and (c) one period of grating

where

$$r = \frac{\bar{n}_I - \bar{n}_{II}}{\bar{n}_I + \bar{n}_{II}}, \quad t = \sqrt{1 - r^2}, \quad \tilde{\beta}_I = \omega \bar{n}_I / c - j\alpha_3 / 2, \quad \tilde{\beta}_{II} = \omega \bar{n}_{II} / c - j\alpha_3 / 2 \quad (11)$$

\bar{n}_I and \bar{n}_{II} are the refractive indices of corrugation. The overall transfer matrix of the Bragg section consisting of M periods is obtained by

$$T_G = \prod_{i=1}^M [T] \quad (12)$$

The effect of facet reflectivity is considered via multiplying T_G by appropriate matrix describes the facet reflectivity at the right end. The reflection of the DBR section is given by

$$r_{DBR} = \frac{T_{G21}}{T_{G11}} \quad (13)$$

where T_{G21} and T_{G11} are the elements of the overall transfer matrix of DBR section.

Dominant oscillating mode is obtained by using the rate equation determining the carrier densities in the DBR sections along with appropriate relations describing the carrier induced index and absorption variations [6], [9], [18]. The carrier densities are related to the injection current densities by rate equations:

$$\frac{dN_1}{dt} = \frac{J_1}{ed_1} - N_1 \left(\frac{1}{\tau_s} + B_1 N_1 + C_1 N_1^2 \right) - v_g A_0 (N_1 - N_0) (1 - \epsilon P) \quad (14)$$

$$\frac{dP}{dt} = v_g \Gamma_1 A_0 (N_1 - N_0) (1 - \varepsilon P) P - v_g (2\alpha'_{th} + \alpha_0) P \quad (15)$$

$$\frac{dN_i}{dt} = \frac{J_i}{ed_i} - N_i \left(\frac{1}{\tau_s} + B_2 N_i + C_2 N_i^2 \right), \quad i = 2, 3 \quad (16)$$

with J_1 , J_2 , J_3 are the current densities in the active, phase and grating sections, respectively. e is the electronic charge, d_1 is the active layer thickness, v_g is the group velocity in the active section, A_0 is the gain/carrier density slope, N_0 is the transparency carrier density, ε is the gain compression factor, S is the photon density distribution in the active region, τ_s is the linear recombination time, B_1 and B_2 are the bimolecular recombination coefficient and C_1 and C_2 are the Auger recombination coefficient in the active and passive sections, respectively. P represents the uniform photon density along the active section. By considering the effect of injection current to the phase and grating sections, the oscillation condition becomes

$$\Gamma_1 g_1 = (2\alpha'_{th} + \alpha_1) = \Gamma_1 A_0 (N_1 - N_0) \quad (17)$$

α'_{th} is threshold gain for a given injected current density J_2 or J_3 . The photon density P inside the active region can be determined by (14) and (17). The features of numerical processing, for tracing the main mode of oscillation, can be described as follows.

The oscillation parameters ($\omega_{th}^m, \alpha_{th}^m$) are calculated at threshold with zero injected current in all passive sections. By applying I_{PC} and I_{DBR} , refractive index and absorption coefficient of passive sections are modified and new oscillation condition is calculated. The photon density of main mode is altered by (14) and (17) and then new refractive index of active region is calculated. The new refractive index of refraction n_1 is introduced in the model and the oscillation parameters are computed again, this procedure is repeated until a point of convergence is reached where the net threshold gains and lasing wavelengths change no more. Finally, the wavelength and output power of the main mode of oscillation are calculated. Fig. 4. shows wavelength tuning curves for dominant mode. The flow-chart of numerical process for tracing of dominant mode is shown in Fig. 3. The value of the material and structure parameters of laser used in this case is derived from [6], [9].

3. PHOTON DENSITY DISTRIBUTION

The algorithm for calculation of photon density distribution is the same as the method that presented by Orafanos et al [16] and Chu et al [21], for the study of photon density distribution in DFB laser and SOA. A critical point for calculating of Photon density distribution, is the introduction of boundary conditions (reflectivity's) at the ends of the structure, since they strongly affect the solution. Reflectivity's can be included by using an adequate matrix, which at the right end takes the form [Fig. 1.]:

$$\begin{bmatrix} U_1 \\ V_1 \end{bmatrix} = [T_{facet}] \cdot \begin{bmatrix} U_0 \\ V_0 \end{bmatrix} \quad (18)$$

$$T_{facet} = \frac{1}{\sqrt{1-r_1^2}} \begin{bmatrix} 1 & r_1 \\ r_1 & 1 \end{bmatrix} \quad (19)$$

where U_1 , V_1 are the waves in the cavity just after the reflectivity; U_0 , V_0 are the output waves at the right end of the cavity; and r_1 is the magnitude of the right facet reflectivity.

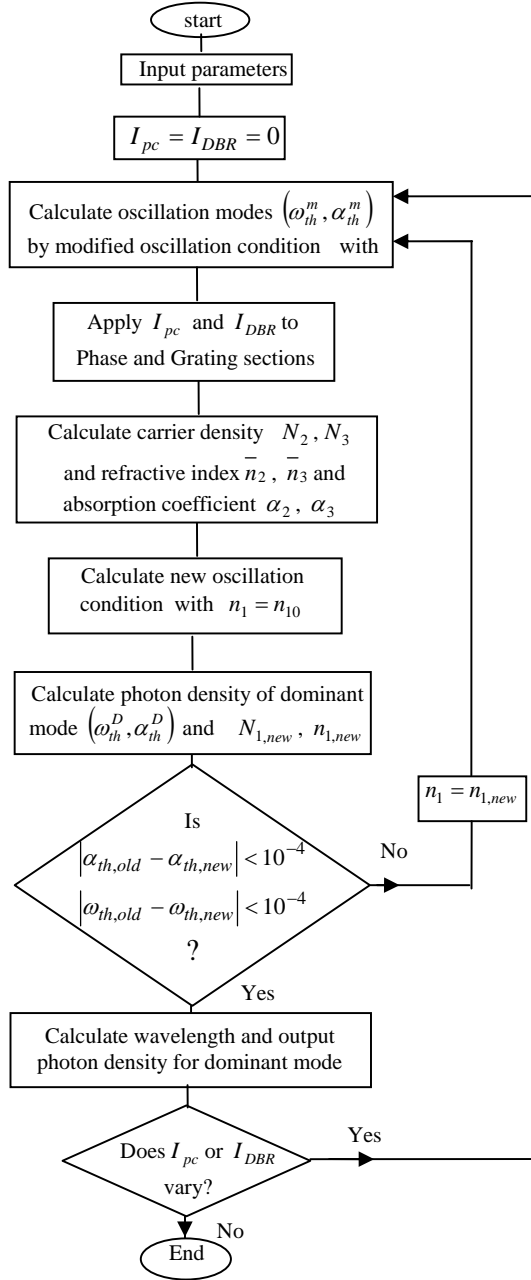
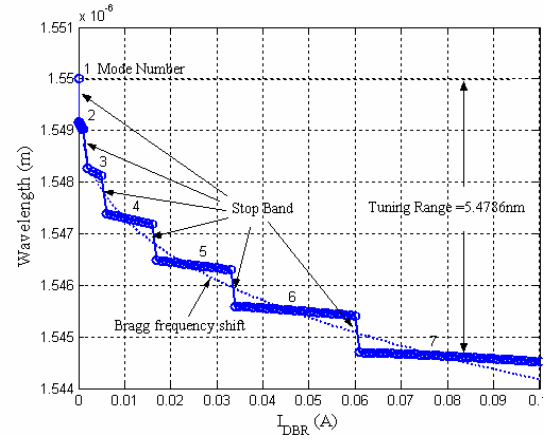
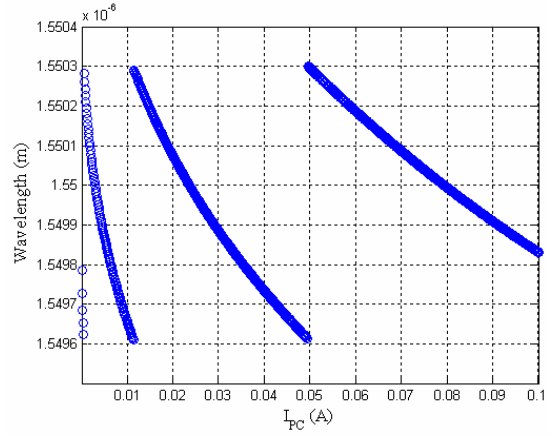


Figure 3: Flow-chart for investigating tuning characteristics



(a)



(b)

Figure 4: Tuning curves for the dominant mod as function of (a) DBR current, (b) Phase current

The transfer matrix for the gain section, as shown in Fig. 1, is given simply by the product of transfer matrices for homogeneous waveguides. The transfer matrix $T_{k,tot}$ at the left end of the k_{th} subsection is defined by

$$\begin{bmatrix} U_k \\ V_k \end{bmatrix} = \underbrace{[T_{k-1} \times T_{k-2} \times \dots \times T_1]}_{T_{k,tot}} \cdot [T_{facet}] \cdot \begin{bmatrix} U_0 \\ V_0 \end{bmatrix} \quad (20)$$

where

$$\begin{bmatrix} U_k \\ V_k \end{bmatrix} = [T_{k-1}] \cdot \begin{bmatrix} U_{k-1} \\ V_{k-1} \end{bmatrix} \quad (21)$$

$$T_{k-1} = \begin{bmatrix} \exp(j\tilde{\beta}_{th}^{k-1} \Delta z) & 0 \\ 0 & \exp(-j\tilde{\beta}_{th}^{k-1} \Delta z) \end{bmatrix} \quad (22)$$

$\tilde{\beta}_{th}^{k-1}$ is complex propagation constant in active region, and defined by the algorithm that presented in[1], [9]. For oscillation in laser we don't have any input, by taking $V_0 = 0$, one obtains

$$U_k = T_{k,tot} (1,1) U_0 \quad (23)$$

$$V_k = T_{k,tot} (2,1) U_0$$

The photon density at the end of k_{th} subsection is then given by

$$P_k = \frac{P_L}{|U_0|^2} (|U_k|^2 + |V_k|^2) = P_L (|T_{k,tot} (1,1)|^2 + |T_{k,tot} (2,1)|^2) \quad (24)$$

P_L being the normalization constant to be determined [9]. The relationship between the $\begin{bmatrix} U_i \\ V_i \end{bmatrix}$ and $\begin{bmatrix} U_{i-1} \\ V_{i-1} \end{bmatrix}$ in phase section is

$$\begin{bmatrix} U_i \\ V_i \end{bmatrix} = \begin{bmatrix} \exp(j\tilde{\beta}_{pc}^{i-1} \Delta z) & 0 \\ 0 & \exp(-j\tilde{\beta}_{pc}^{i-1} \Delta z) \end{bmatrix} \begin{bmatrix} U_{i-1} \\ V_{i-1} \end{bmatrix} \quad (25)$$

where

$$\tilde{\beta}_{pc}^{i-1} = \frac{\omega_{th} \bar{n}_2}{c} - j \frac{\alpha_2}{2} \quad (26)$$

$\tilde{\beta}_{pc}^{i-1}$ is complex propagation constant in phase region. ω_{th} is dominant mode frequency. \bar{n}_2 and α_2 are the refractive index and loss coefficient in phase section. The relationship between fields in the Bragg grating section is [Fig. 2.],

$$\begin{bmatrix} U_j \\ V_j \end{bmatrix} = \frac{1}{t} \begin{bmatrix} 1 & r \\ r & 1 \end{bmatrix} \begin{bmatrix} e^{j\tilde{\beta}_h^{j-1} l} & 0 \\ 0 & e^{-j\tilde{\beta}_h^{j-1} l} \end{bmatrix} \frac{1}{t} \begin{bmatrix} 1 & -r \\ -r & 1 \end{bmatrix} \begin{bmatrix} e^{j\tilde{\beta}_l^{j-1} l} & 0 \\ 0 & e^{-j\tilde{\beta}_l^{j-1} l} \end{bmatrix} \begin{bmatrix} U_{j-1} \\ V_{j-1} \end{bmatrix} \quad (27)$$

The flow-chart of model for calculation of photon density is shown in Fig. 5.

4. RESULTS AND DISCUSSION

In Fig. 6. and 7., we present the Photon density distribution in different sections of cavity, for several values of the phase and Bragg injection currents. A little variation of the refractive index in the active region due to injection current to passive sections, caused to a curvature shape in photon density distribution profile. The point at which the distribution peaks, correspond to the interfaces between the different sections. In Fig. 6. the effect of I_{DBR} is investigated. High injection current is caused downward shift of profile. Because by Increasing I_{DBR} , Bragg frequency and grating loss are increased. As shown in Fig. 7., photon density is more sensitive to phase current than grating current.

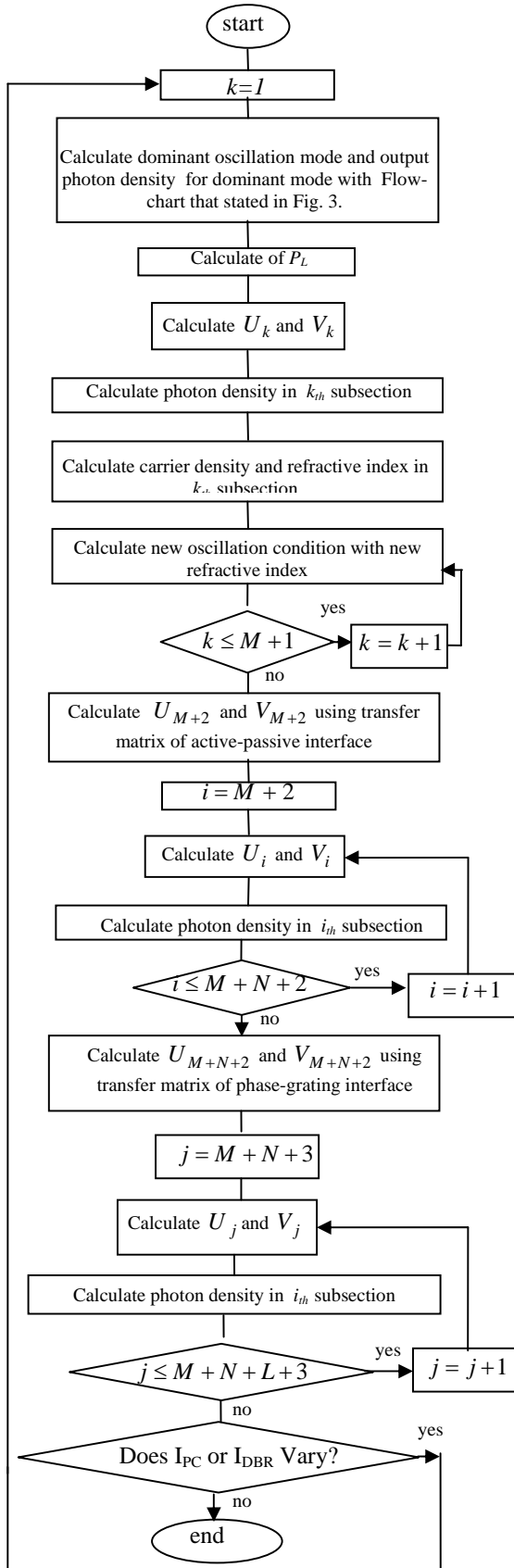


Figure 5: Photon density distribution algorithm

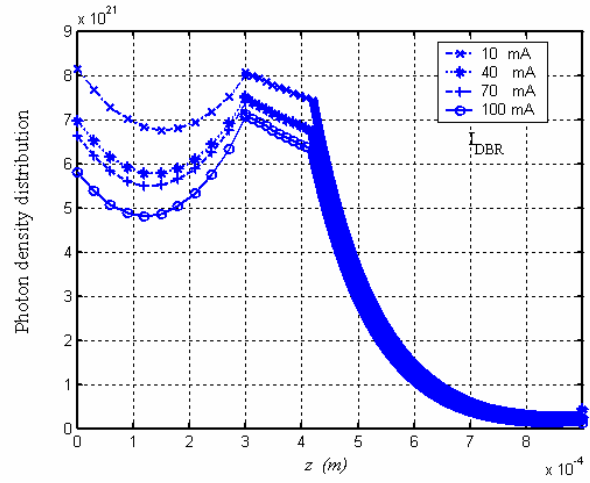


Figure 6: Longitudinal distribution of photon density in a three-section DBR laser for different values of grating current

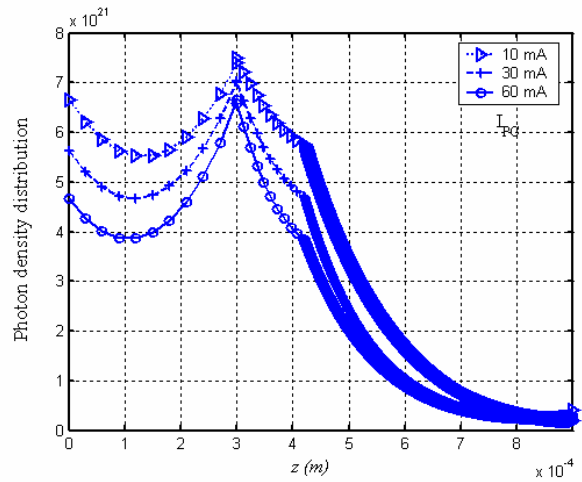


Figure 7: Longitudinal distribution of photon density in a three-section DBR laser for different values of phase current

5. CONCLUSION

A model based on the transfer matrix method for calculation photon density distribution is developed and described. Photon density profile in each laser section is simulated and the effect of injection current to gratig and phase section on photon density profile is investigated. It is shown that injection currents are caused downward shift in photon density distribution profile.

ACKNOWLEDGEMENT

This work is partially supported by the Iran Telecommunication Research Center (ITRC).

REFERENCES

1. L. A. Coldren, G. A. Fish, Y. Akulova, J. S. Barton, L. Johansson and C. W. Coldren, "Tunable Semiconductor Lasers: A Tutorial," *IEEE J. Lightwave Technol.*, vol. 22, pp. 193-202, 2004.
2. L. A. Coldren, "Monolithic Tunable Diode Lasers," *J. on Selected Topics in Quantum Electron.*, vol. 6, pp. 988-999, 2000.
3. E. Bruce, "Tunable Lasers," *IEEE Spectrum*, February, 2002.
4. T. L. Koch and U. Koren, "Semiconductor Lasers for Coherent Optical Fiber Communications," *IEEE J. Lightwave Technol.*, vol. 8, pp. 274-293, 1990.
5. K. Komori, S. Arai, Y. Suematsu, I. Arima and M. Aoki. "Single-Mode Properties of Distributed-Reflector Lasers," *IEEE J. Quantum Electron.*, vol. 25, pp. 1235-1244, 1989.
6. X. Pan, H. Olesen and B. Tromborg " A Theoretical Model of Multielectrode DBR Lasers," *IEEE J. Quantum Electron.*, Vol. 24, pp. 2423-2432, 1988
7. E. Patzak, P. Meissner and D. Yevick, "An Analysis of the Linewidth and Spectral Behavior of DBR Lasers," *IEEE J. Quantum Electron.*, vol. QE-21, No. 9, pp. 1318-1325, 1985.
8. N. P. Caponio, M. Goano, I. Maio, M. Meliga, G. P. Bava, G.D. Anis and I. Montrosset "Analysis and Design Criteria of Three-Section DBR Tunable Lasers," *IEEE J. on Selected Areas in Commun.*, vol 8, pp.1203-1213, 1990.
9. A. Tsgopoulos, T. Sphicopoulos, I. Orfanos and S. Pantelis "Wavelength Tuning Analysis and Spectral Characteristics of Three-Section DBR Lasers," *IEEE J. Quantum Electron.*, vol. 28, pp. 415-426, 1992
10. L. G. Kazovsky, M. Stern, S. G. Menocal and C. Zah, " DBR Active Optical Filters: Transfer Function and Noise Characteristics," *IEEE J. Lightwave Technol.*, vol. 8, pp.1441-1450, 1990.
11. M. Teshima, " Dynamic Wavelength Tuning Characteristics of the 1.5- μm Three-Section DBR Lasers: Analysis and Experiment," *J. Quantum Electron.*, vol.31, pp. 1389-1400 , 1995.
12. M. H. Yavari, V. Ahmadi, F. Shahshahani, " Numerical Analysis of Three Section Distributed Bragg Reflector Tunable Laser Diode with Modified Oscillation Condition Based on the Transfer Matrix", 21FIP conference on wireless and optical communication systems, IEEE, 2005.
13. M. H. Yavari, *Analysis of semiconductor tunable laser diode and tuning characteristics*, Master of science thesis, Tarbiat Modares University, Iran, 2004.
14. G. Bjork and O. Nilsson, "A New Exact and Efficient Numerical Matrix Theory of Complicated Laser Structures; Properties of Asymmetric Phase-Shifted DFB Lasers," *J. Lightwave Technol.*, vol. LT-5, pp. 140-146, 1987.
15. J. Hong, W. Huang and T. Makino, "On the Transfer Matrix Method for Distributed-Feedback Waveguide Devices," *J. Lightwave Technol.*, vol.10, pp.1860-1868, December, 1992.
16. I. Orfanos, T. Sphicopoulos, A. Tsigopoulos, C. Caroubalos, "A Tractable Above-Threshold Model for the Design of DFB and Phase-Shifted DFB Lasers," *IEEE J. Quantum Electron.*, vol. 27, pp. 946-956, 1991.
17. L. A. Coldren and S.W Corzine, *Diode Lasers and Photonic Integrated Circuits*. John wiley and Sons, California, 1995.
18. M. G. Davis and R. F. O'Dowd, "A New Large-Signal Dynamic Model for Multielectrode DFB Lasers Based on the Transfer Matrix Method," *IEEE Photonic Technol. Lett.*, vol. 4, pp. 838-840 , 1992.
19. M. C. Amann and J. Buss, *Tunable Laser Diodes*. London, Artech House, 1998.
20. B. Tromborg, H. Olesen, X. Pan, and S. Satio " Transmission Line Description of Optical Feedback and Injection Locking for Fabry-Perot and DFB Lasers," *IEEE J. Quantum Electron.*, vol. QE-23, pp. 1875-1889, 1987.
21. C. Y. J. Chu and H. Ghafouri-shiraz, "Analysis of Gain and Saturation Characteristics of a Semiconductor Laser Optical Amplifier Using Transfer Matrices," *IEEE J. Lightwave Technol.*, vol. 12, pp. 1378-1386, 1994.